
 PHYSICAL METHODS FOR INVESTIGATION
 OF CHEMICAL PROCESSES

Experimental and Theoretical Studies on the Synthesis, Electronic Structure and Biphasic Extraction Properties of Functionalized Thia-Crown Ethers

B. Çiçek^a (ORCID: 0000-0003-1257-1188), A. Ergün^a (ORCID: 0000-0003-4647-6058),
 Ü. Çalışır^b (ORCID: 0000-0001-7699-2008), and A. Azizoglu^{a,*} (ORCID: 0000-0002-5098-1842)

^a Balıkesir University, Chemistry Department, Faculty of Science and Arts, Çağış Campus, Balıkesir, TR-10145 Türkiye

^b Siirt University, Science and Technology Application & Research Centre, Kezer Campus, Siirt, TR-56100 Türkiye

*e-mail: azizoglu@balikesir.edu.tr

Received June 29, 2025; revised November 16, 2025; accepted November 20, 2025

Abstract—In the present study, three thia-crown ether derivatives (**AE1**, **AE2**, **AE3**) were synthesized using diacyl chlorides and tri(ethylene glycol) dithiol, and characterized by infrared, proton nuclear magnetic resonance, and mass spectrometry. Their metal complexation properties with K^+ , Na^+ , Ag^+ , Ca^{2+} , Mg^{2+} , Zn^{2+} , and Fe^{2+} were investigated using liquid–liquid ion-pair extraction in chloroform and dichloromethane. Extraction efficiencies, equilibrium constant, and Gibbs free energies were calculated. **AE1** and **AE2** exhibited the highest extraction efficiencies for K^+ and Zn^{2+} (>95%), whereas Na^+ and Ca^{2+} showed the lowest. The solvent type significantly influenced extraction selectivity, with dichloromethane enhancing K^+ selectivity. The results correlated well with the hard–soft acid–base principle, where **AE3**, having the highest hardness, favored harder metal ions, while **AE1** and **AE2**, being softer, preferred softer or borderline cations. Density Functional Theory calculations supported the experimental findings, providing insights into ligand electronic structures through frontier molecular orbital energy gaps and global hardness values. The study demonstrates that structural differences among ligands and solvent polarity critically affect metal ion selectivity and efficiency.

Keywords: thia-crown ether, extraction, in silico, complexation

DOI: 10.1134/S1990793125701763

INTRODUCTION

Macrocyclic compounds, particularly crown ethers, have long attracted scientific attention due to their ability to selectively complex with metal ions through size-matching and donor atom interactions [1–4]. Among these, thiacyclic ligands—macrocyclic ligands that incorporate sulfur donor atoms—have demonstrated significant potential in coordination chemistry due to their high affinity toward soft and borderline metal cations as predicted by the Hard and Soft Acids and Bases (HSAB) theory [5–7]. Although thiacyclic ligands have been known since the 1970s [8], their exceptional capacity for metal ion complexation has been more fully explored in recent years [9–12]. The introduction of sulfur atoms into macrocyclic frameworks enhances their selectivity for soft Lewis acids such as Ag^+ and Hg^{2+} , while also improving lipophilicity and electron-donating capability compared to their oxygen-containing counterparts [13, 14]. These structural features render thia-crown ethers of potential interest for the development of liquid–liquid extraction systems, metal ion sensors, and biological enzyme modulators [12, 15].

Previous investigations have shown that macrocyclic sulfur ligands demonstrate promising extraction

capabilities for various transition metal ions under biphasic conditions, especially when combined with polar organic solvents such as chloroform or dichloromethane [16]. Furthermore, the substitution pattern of donor atoms, ring size, and heteroatom distribution are known to significantly influence metal ion selectivity [17, 18].

In parallel, Density Functional Theory (DFT) calculations have emerged as a reliable method for predicting the electronic structure, reactivity, and hardness parameters of ligands, thereby enabling deeper insight into ligand–metal interactions [19–22]. According to the HSAB principle, the binding affinity between a metal ion and a ligand can be rationalized based on their respective hardness (η) values, where better hardness compatibility leads to more stable complex formation [5].

This study focuses on the synthesis, structural characterization, and complexation behavior of three newly synthesized thia-crown ether derivatives—**AE1**, **AE2**, and **AE3**—toward environmentally and biologically relevant metal ions. The complexation properties were examined via liquid–liquid ion-pair extraction in two solvent systems, and correlated with DFT-calculated electronic parameters and HSAB-based inter-

pretations. This combined experimental and theoretical approach aims to advance the fundamental understanding of structure–activity relationships in sulfur-containing macrocyclic ligands, providing insights that could inform the future design of systems for selective metal ion recognition and separation.

EXPERIMENTAL AND THEORETICAL DETAILS

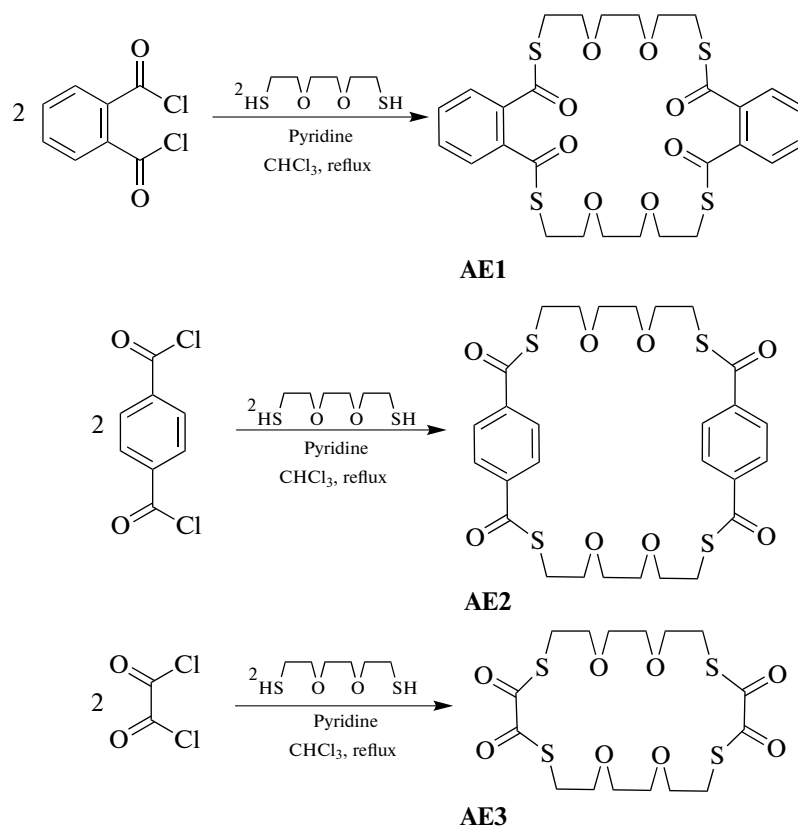
Materials

All chemicals, solvents, and materials employed in this study were of analytical grade and sourced from established suppliers, including Merck, Sigma-Aldrich, Alfa Aesar, and Fluka Co. Laboratory glassware, including volumetric flasks and beakers, as well as other equipment, were provided by ISOLAB. Melting points were determined using an Electrothermal 9200 melting point apparatus. Fourier transform infrared (FTIR) spectra were recorded on a Perkin Elmer Spectrum 100 FTIR spectrometer, while proton nuclear magnetic resonance ($^1\text{H-NMR}$) spectra were acquired using a Varian 400 MHz spectrometer. Mass spectrometry analysis was performed using a Shimadzu GSMS–QP2010 spectrometer. Column chromatography was conducted with Merck silica gel 60 (230–400 mesh ASTM). All solvents were dried according to standard procedures. The benzo-thia-

crown ethers (**AE1**–**AE3**) were prepared as 10^{-3} M stock solutions in dichloromethane and chloroform. Following the extraction process, the concentrations of metal ions were quantified using inductively coupled plasma optical emission spectrometry (ICP-OES) (Perkin Elmer Optima 3100 XL) at ambient temperature. The metal ion extraction procedure was carried out based on previously established methodologies [16].

Syntheses of Thia-Crown Ethers

Using diacyl chloride (diacylphthaloyl dichloride and oxalyl dichloride) and tri(ethylene glycol) dithiol in the presence of a pyridine base, macrocyclic three thiacycrown ethers, designated **AE1**, **AE2**, and **AE3**, were synthesized in the current study (see Scheme 1). Their syntheses and characterization details were described in a previous one [12]. To synthesize thia-crown ethers, *o*-phthaloyl dichloride, *p*-phthaloyl dichloride or oxalyl dichloride (30 mmol), along with 2,2'-(ethylenedioxy)diethanethiol (30 mmol), and pyridine (60 mmol), were dissolved in chloroform. The mixtures were stirred and subjected to reflux under a nitrogen atmosphere for 24 h. Following the reaction, the solvents were removed by evaporation, and the resulting products were purified using silica gel chromatography with an *n*-hexane–chloroform mixture as the eluent.



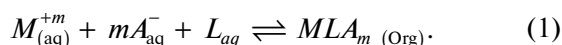
Scheme 1. Syntheses of thiacrown ethers, **AE1**, **AE2**, and **AE3**.

Liquid–Liquid Ion-Pair Metal Extraction Studies

The liquid–liquid ion-pair extraction technique is widely employed for the selective transfer of metal ions from an aqueous phase to an immiscible organic phase. This method involves the formation of an ion-pair complex between a metal-crown ether cationic complex and its counter anion, which facilitates its solubility and transfer into the organic solvent. In this study, chloroform and dichloromethane were utilized in this study due to their halogenated nature, moderate polarity, and immiscibility with water, which collectively enhance phase separation efficiency [23]. Although chlorinated solvents pose environmental and health risks, the ligands synthesized herein are highly soluble in these solvents, which justifies their use. The extraction equilibrium constant (K_{ext}) can be quantitatively expressed by the following thermodynamic relationship.

Theoretical Framework

Liquid–liquid extraction involves the partitioning of inorganic species into an organic phase through the interaction of two immiscible liquids—typically an aqueous (inorganic) phase containing metal salts, and an organic phase composed of solvents such as dichloromethane, diethyl ether, chloroform, or benzene, which may contain organic ligands. The theoretical basis and associated equations used in this study are adapted from Çakir et al. [16], and can be outlined as follows:



In this expression, $M_{(\text{aq})}^{+m}$ is the metal ion in the aqueous phase at equilibrium, m represents the stoichiometric number of anions required to neutralize the metal–ligand complex, $A_{(\text{aq})}^{-}$ is the counter anion, and $L_{(\text{aq})}$ is the ligand present in the aqueous phase. The product $MLA_m_{(\text{Org})}$ represents the resulting metal–ligand–anion complex transferred into the organic phase as a result of the extraction.

The corresponding extraction equilibrium constant, K_{ext} , which quantifies the extent of the extraction process, is defined in terms of species concentrations at equilibrium:

$$K_{\text{ext}} = \frac{[MLA_m]_{\text{Org}}}{[M^{+m}]_{\text{aq}}[A^{-}]_{\text{aq}}^m[L]_{\text{aq}}}, \quad (2)$$

where the aqueous-phase equilibrium concentrations of the metal ion, anion, and ligand are given by $[M^{+m}]_{\text{aq}}$, $[A^{-}]_{\text{aq}}$, and $[L]_{\text{aq}}$, respectively. This thermodynamic constant provides a quantitative measure of the extent to which the metal–ligand–anion complex is favored in the organic phase.

For practical evaluation of extraction performance, the extraction efficiency (Ext%) is calculated as

$$\text{Ext}\% = 100 \times \left([MLA_m]_{\text{Org}} / [M_0^{+m}]_{\text{aq}} \right), \quad (3)$$

where $[M_0^{+m}]_{\text{aq}}$ represents the initial concentration of the metal ion prior to extraction. Thus, Ext% directly reflects the proportion of metal transferred from the aqueous phase.

Similarly, the distribution coefficient,

$$K_D = [MLA_m]_{\text{Org}} / [M^{+m}]_{\text{aq}}, \quad (4)$$

describes the partitioning of the metal species between the organic and aqueous phases at equilibrium and is commonly used to compare extraction efficiencies among different metal ions.

Thermodynamic feasibility of the extraction process is evaluated through the standard Gibbs free energy change ($\Delta G_{\text{ext}}^{\circ}$), calculated using:

$$\Delta G_{\text{ext}}^{\circ} = -RT \ln(K_{\text{ext}}). \quad (5)$$

A negative value of $\Delta G_{\text{ext}}^{\circ}$ indicates that the extraction process is spontaneous under standard conditions ($R = 8.314 \text{ J mol}^{-1} \text{ K}^{-1}$; $T = 298 \text{ K}$), confirming the thermodynamic favorability of the system [24].

Additionally, the selectivity factor, $S_{f(\text{ion } 1)}$, between two competing metal ions (ion 1 and ion 2) is defined as

$$S_{f(\text{ion } 1)} = (K_{D(\text{ion } 1)} / K_{D(\text{ion } 2)}), \quad (6)$$

providing a comparative metric for the ligand's preference toward one metal ion over another.

This study extends prior work on thia-crown ethers [10, 12, 16] by employing a competitive extraction approach to quantify and compare the extraction constants (such as K_{ext} , Ext%, $\Delta G_{\text{ext}}^{\circ}$, etc.) for a wide range of metal ions under identical conditions. Furthermore, we provide a systematic examination of the interplay among the macrocyclic structure of the ligands, the HSAB principle [5, 6], and solvent effects [17, 18]. The analysis of the findings highlights the significance of metal ion chemical hardness and ionic radius in interpreting the results. This combined methodology provides a more profound understanding of the structure–property relationships governing selective metal ion recognition in thia-crown ether systems.

In the experiment, a liquid-liquid ion-pair extraction was conducted using an aqueous solution containing seven different metal ions (each at a concentration of $10^{-3} \text{ mol L}^{-1}$) and thia-crown ethers (also at $10^{-3} \text{ mol L}^{-1}$), with each extraction performed separately. The prepared mixtures were agitated at 300 rpm for one hour using an orbital shaker, followed by a 30-min incubation period at 25°C to ensure complete equilibration of the system. The low concentra-

tion conditions prevented any observable precipitation formation. Following phase separation, quantitative analysis of residual metal ion concentrations in the aqueous phase was performed by ICP-OES. These measurements enabled the determination of key thermodynamic parameters: the extraction constant (K_{ext}), extraction efficiency (Ext%), logarithmic extraction equilibrium constant ($\log K_{\text{ext}}$), and standard Gibbs free energy change ($\Delta G_{\text{ext}}^{\circ}$) for the process.

Quantum Chemical Methods and Programs of Theoretical Calculations

In this work we performed quantum chemical calculations to gain insight into the structural and electronic properties of the **AE1**–**AE3** compounds. All computations were carried out using Density Functional Theory (DFT) as implemented in the Gaussian 09 software package [25]. The geometries of title compounds were optimized in the gas phase without imposing symmetry constraints, employing the B3LYP functional in conjunction with the 6-31G+(d) basis set for all atoms [26, 27]. This level of DFT is well-regarded for its high accuracy in predicting molecular geometries and electronic properties [28–32].

Frequency calculations were also conducted at the same level of theory to ensure that the optimized structures correspond to true minima on the potential energy surface [33]. In order to investigate the electronic properties, including frontier molecular orbital (HOMO–LUMO) energies, ionization potential (I), electron affinity (A), chemical hardness (η) and softness (S), electronegativity (χ), and dipole moments (μ) [29, 31], supplementary single-point energy calculations were carried out at the B3LYP/6-31G+(d) level of theory.

RESULTS AND DISCUSSION

In the present study, a new set of macrocyclic thiacyclic ethers, namely **AE1**, **AE2**, and **AE3**, were synthesized by utilizing diacyl chloride (diacylphthaloyl dichloride and oxalyl dichloride) and tri(ethylene glycol) dithiol in the presence of a pyridine base. The synthetic protocol was performed according to the established procedure [12], with modifications as described in the experimental section. Upon completion of the synthesis, the isolated compounds were characterized using a combination of spectroscopic and analytical techniques, including $^1\text{H-NMR}$ spectroscopy, FTIR spectroscopy, and gas chromatography–mass spectrometry (GC-MS). The experimental proton NMR and FTIR spectra for compounds **AE1**–**AE3** can also be found in the Supplementary Information (Figs. SI-1–SI-3). In the experimental FTIR spectra of title compounds (Figs. SI-4–SI-6), a bending vibration of the C–S–C group was detected at around 680 cm^{-1} , the O=C–S stretching was observed

in the range of $1700\text{--}1720\text{ cm}^{-1}$, and the aromatic C=C stretching occurred between $1630\text{--}1640\text{ cm}^{-1}$. These distinctive IR peaks and modes were also observed and confirmed through theoretical vibrational analyses at the B3LYP/6-31G+(d) level (Figs. SI-7–SI-9). A detailed listing of the calculated FTIR peak positions for **AE1**, **AE2**, and **AE3** is provided in Tables SI-1–SI-3, which summarizes the corresponding vibrational frequencies (cm^{-1}) and molar absorptivity values ($\epsilon, \text{M}^{-1}\text{ cm}^{-1}$). In particular, bending vibration of the C–S–C group for **AE1**, **AE2**, and **AE3**, are calculated to be $679, 677,$ and 676 cm^{-1} , respectively. The calculated stretching vibrational frequencies of the O=C–S group are $1733\text{--}1759\text{ cm}^{-1}$ for **AE1**, $1733\text{--}1762\text{ cm}^{-1}$ for **AE2**, and $1756\text{--}1776\text{ cm}^{-1}$ for **AE3**. Lastly, the aromatic C=C stretching vibrations were computed in the range of $1618\text{--}1643\text{ cm}^{-1}$ for **AE1** and $1652\text{--}1653\text{ cm}^{-1}$ for **AE2**. The $^1\text{H-NMR}$ spectra of **AE1**, **AE2**, and **AE3**, exhibited chemical shifts between 2.4 and 2.45 ppm, corresponding to the hydrogen atoms on the C–S–C=O framework. The hydrogen atoms attached to aromatic rings also showed chemical shifts between 6.55 and 8.15 ppm.

Following the characterization of the synthesized compounds **AE1**–**AE3**, their metal ion extraction capabilities were systematically evaluated using liquid-liquid ion-pair extraction techniques. The extraction experiments were conducted in biphasic systems consisting of dichloromethane/water (50 : 50; v/v) and chloroform/water (50 : 50; v/v), focusing on the selective extraction of K^+ , Ca^{2+} , Na^+ , Ag^+ , Fe^{2+} , Zn^{2+} , and Mg^{2+} ions. Table 1 summarizes the data obtained from the liquid-liquid extraction experiments, which were conducted in accordance with the procedures outlined in the part of materials and methods. The liquid-liquid ion-pair extraction process involves complex formation between the organic-phase ligand (L) and aqueous-phase metal cation (M^{+m}), as described by the equilibrium reaction (Eq. (1)). The extraction efficiency, quantified as the percentage of metal ions transferred to the organic phase, serves as a direct measure of complexation stability. Elevated extraction percentages reflect favorable complex formation and strong ligand-metal coordination thermodynamics.

The extraction constants K_{ext} and K_{D} , determined using Eqs. (2) and (4), reflect the system's extraction performance. Larger values of these constants correspond to higher extraction efficiency. Due to the large magnitude of the obtained data, they are presented in logarithmic form. When examining the $\log(K_{\text{ext}})$ values obtained for the extraction of K^+ , Ca^{2+} , Na^+ , Ag^+ , Fe^{2+} , Zn^{2+} , and Mg^{2+} ions by the **AE1**, **AE2**, and **AE3** compounds in the chloroform solvent system, it was observed that the K^+ , Zn^{2+} , and Ag^+ ions exhibited relatively high complexation and higher extraction efficiencies. In CH_2Cl_2 , while the **AE1** compound similarly exhibited relatively high complexation with

Table 1. The liquid-liquid extraction of K^+ , Ag^+ , Na^+ , Ca^{2+} , Fe^{2+} , Zn^{2+} , and Mg^{2+} ions (with their respective ionic radii in pm) by **AE1**, **AE2**, and **AE3**. The calculated values of $\log(K_{ext})$, extraction efficiency (Ext%), and standard Gibbs free energy change of extraction (ΔG_{ext}°) for biphasic $CHCl_3 : H_2O$ (50:50) and $CH_2Cl_2 : H_2O$ (50 : 50) systems under natural pH conditions at 25°C

Crown Ether	Ion	Ion radius, pm*	$\log(K_{ext})$		Ext %		$(-)\Delta G_{ext}$	
			$CHCl_3 : H_2O$ (50%)	$CH_2Cl_2 : H_2O$ (50%)	$CHCl_3 : H_2O$ (50%)	$CH_2Cl_2 : H_2O$ (50%)	$CHCl_3 : H_2O$ (50%)	$CH_2Cl_2 : H_2O$ (50%)
AE1	K^+	138	18.1786	19.7092	95.9	99.5	24785.0	26871.9
	Ag^+	115	17.6096	18.1936	92.7	96.0	24009.4	24805.5
	Na^+	102	12.5650	13.1953	43.4	56.7	17131.4	17990.8
	Ca^{2+}	100	12.8481	12.5632	52.9	43.1	17517.4	17128.9
	Fe^{2+}	76	13.7342	13.8120	69.7	69.3	18725.5	18831.6
	Zn^{2+}	74	18.1785	17.8952	95.9	97.1	24785.0	24398.7
	Mg^{2+}	72	13.5630	13.6448	67.4	66.8	18492.1	18603.6
AE2	K^+	138	18.1509	19.7995	98.2	99.5	24747.3	26995.1
	Ag^+	115	18.2094	14.2757	95.5	69.8	24827.1	19463.8
	Na^+	102	12.0071	11.7712	28.4	16.7	16370.7	16049.1
	Ca^{2+}	100	13.6202	12.4165	69.8	35.9	18570.1	16928.9
	Fe^{2+}	76	13.8454	13.9196	72.4	69.6	18877.2	18978.2
	Zn^{2+}	74	18.1509	16.8558	98.2	94.9	24747.3	22981.5
	Mg^{2+}	72	13.5956	14.1250	68.6	73.1	18536.6	19258.4
AE3	K^+	138	16.9846	19.7427	96.7	99.5	23157.2	26917.6
	Ag^+	115	17.4716	15.7793	91.9	91.5	23821.1	21513.8
	Na^+	102	12.6132	12.6582	46.7	41.7	17197.1	17258.4
	Ca^{2+}	100	13.7482	12.2371	72.6	34.1	18744.6	16684.3
	Fe^{2+}	76	13.6899	15.8894	70.4	86.7	18665.1	21663.9
	Zn^{2+}	74	16.9846	15.7968	96.7	90.4	23157.2	21537.7
	Mg^{2+}	72	14.4721	14.1978	78.8	73.8	19731.5	19357.6

* Metal ion radius in pm [34].

K^+ , Zn^{2+} , and Ag^+ ions, the **AE2** and **AE3** compounds showed relatively high complexation with K^+ ions. In the 1 : 1 dichloromethane extraction system, the K^+ ion typically exhibited higher extraction efficiency compared to other ions.

The $-\Delta G_{ext}^\circ$ values, which measure the spontaneity of a process, were calculated using Eq. (5) [10]. The obtained negative ΔG_{ext}° values indicate that the extraction is spontaneous. All extractions involving the **AE1**, **AE2**, and **AE3** compounds proceeded spontaneously. Their extraction efficiencies, calculated using Eq. (3), are presented in Table 1. The use of chloroform and dichloromethane as extraction solvents led to distinct differences in the outcomes.

The extraction percentages presented in Table 1 for the extractions conducted using chloroform were carefully examined and analyzed. The **AE1** compound extracted K^+ (95.9%) and Zn^{2+} (95.9%) ions the most, followed by Ag^+ ions (92.7%). The ion with the least complexation by the **AE1** compound was Na^+ ion at 43.4%. According to the extraction percentages given in Table 1, the **AE2** compound could extract K^+ (98.2%) and Zn^{2+} (98.2%) ions the most, while Na^+ ion was extracted the least (28.4%). The **AE2** compound also demonstrated remarkably high extraction efficiency for Ag^+ ions, achieving a rate of 95.5%. The **AE3** compound extracted K^+ and Zn^{2+} ions at 96.7% and Ag^+ ions at 91.9%. The cation with the least extraction by the **AE3** compound was Na^+ cation (46.7%).

Through liquid-liquid ion pair extraction in dichloromethane, the extraction properties of the **AE1**, **AE2**, and **AE3** compounds for the selected ions (K^+ , Ca^{2+} , Na^+ , Ag^+ , Fe^{2+} , Zn^{2+} , and Mg^{2+}) were determined. The extraction percentages provided in Table 1 indicated that the **AE1**, **AE2**, and **AE3** compounds extracted the K^+ ion the most (99.5%). Additionally, it was determined that the **AE1** compound extracted the Ca^{2+} ion the least (43.1%), the **AE2** compound extracted the Na^+ ion the least (16.7%), and the **AE3** compound extracted the Ca^{2+} ion the least (34.1%). The extraction of Ag^+ and Zn^{2+} ions by the **AE1** compound was also very high (96.0 and 97.1%, respectively). The **AE2** compound extracted Zn^{2+} ions (94.9%) significantly, and the **AE3** compound successfully extracted Ag^+ , Fe^{2+} , and Zn^{2+} ions following potassium.

Using the extraction percentages provided in Table 1, the metal ion extractions by the compounds were ranked. The **AE1** compound extracted metal ions in the order of $Zn^{2+} = K^+ > Ag^+ > Fe^{2+} > Mg^{2+} > Ca^{2+} > Na^+$ in chloroform, and $K^+ > Zn^{2+} > Ag^+ > Fe^{2+} > Mg^{2+} > Na^+ > Ca^{2+}$ in dichloromethane. The **AE2** compound extracted metal ions in the order of $Zn^{2+} = K^+ > Ag^+ > Fe^{2+} > Ca^{2+} > Mg^{2+} > Na^+$ in chloroform, and $K^+ > Zn^{2+} > Mg^{2+} > Ag^+ > Fe^{2+} > Ca^{2+} > Na^+$ in dichloromethane. Finally, the **AE3** compound extracted metal ions in the order of $Zn^{2+} = K^+ > Ag^+ > Mg^{2+} > Ca^{2+} > Fe^{2+} > Na^+$ in chloroform, and $K^+ > Ag^+ > Zn^{2+} > Fe^{2+} > Mg^{2+} > Na^+ > Ca^{2+}$ in dichloromethane.

Analysis of the extraction percentages revealed that the synthesized compounds demonstrated high extraction efficiencies for metal ions in the chloroform system, albeit with limited selectivity. In contrast, when dichloromethane was used as the organic phase, the title compounds exhibited enhanced selectivity toward the potassium ion. Additionally, in dichloromethane, the **AE1** and **AE3** compounds showed the lowest extraction efficiency for Ca^{2+} , behavior not observed in the chloroform solvent system. The **AE2** compound demonstrated minimal extraction efficiency towards the sodium ion in dichloromethane, mirroring its extraction profile in chloroform. These findings suggest that solvent polarity plays a critical role in the selectivity and efficiency of metal ion extraction by these thia-crown ether derivatives.

Analysis of the extraction results indicated that all compounds exhibited a notably higher binding affinity for the potassium ion (K^+) within the alkali metal group, while their affinity for the sodium ion (Na^+), another member of the alkali metals, was comparatively reduced. Despite having the same charge, similar hardness, and being in the same group, the reason for the completely different affinities of the compounds is their different radii. As indicated by the

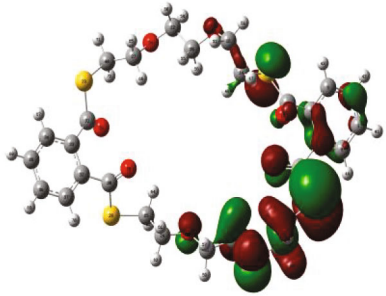
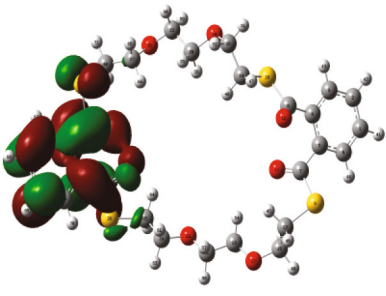
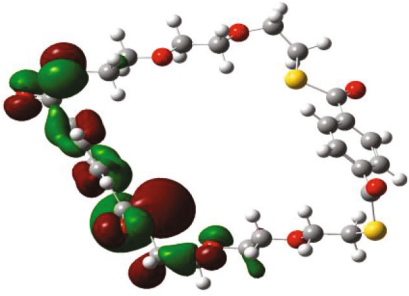
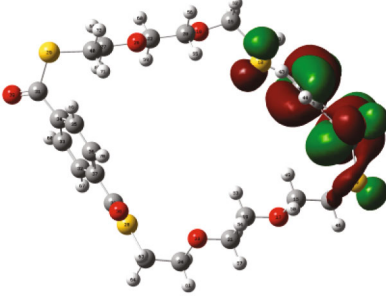
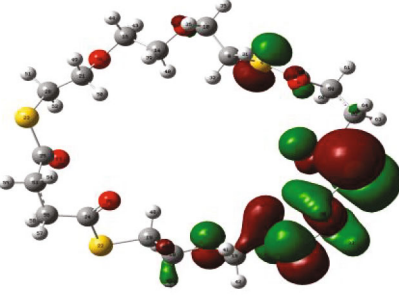
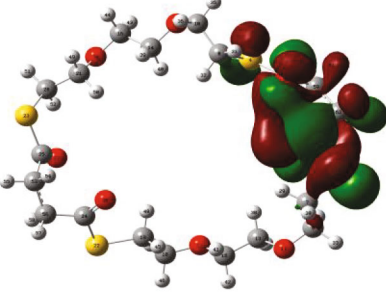
ionic radii data [34] in Table 1, the potassium ion (K^+) exhibits a larger ionic radius relative to the other metal ions examined. Structural analysis of the **AE1**–**AE3** compounds demonstrates that they possess similarly structured hydrophilic inner cavities, owing to an identical number of heteroatoms influencing the cavity geometry. Hence, the metal ion displaying the highest complexation affinity is consistent across all compounds. Although the number of heteroatoms, the number of glycol bridges, and the heteroatom ratio (S/O) are the same, the binding positions of the benzene ring as a side group in the **AE1** and **AE2** compounds are 1,2 and 1,4, respectively. The **AE3** compound lacks a side group; consequently, it exhibited the highest extraction efficiency for the potassium ion, which best fits the ring's internal cavity, whereas the extraction efficiencies for other metal ions varied and showed less consistency. According to the literature, the selective affinity of **AE1**–**AE3** compounds for K^+ among hard Lewis acids, Zn^{2+} among borderline Lewis acids, and Ag^+ among soft Lewis acids highlights the effectiveness of mixed-donor crown ether synthesis. The experimental data further suggest that ionic charge plays a minimal role in influencing complexation behavior.

The O, N, and S donor crown ethers are used as selective extractors of hard-soft metal cations for some enzyme activities [12, 35]. According to Pearson's hard-soft acid-base principle, softness is the opposite of hardness; that is, a low η value means high softness [5]. The principle of hard-soft acids and bases is theoretically derived from the hypothesis that when ionization potentials are the same, additional stability accompanies the ligand's binding to a Lewis acid. Hardness parameters for ligands are calculated using Pearson and Coopmann's theory with the eq. 7 described below [5, 6]:

$$\eta = (E_{LUMO} - E_{HOMO})/2. \quad (7)$$

Hence, we carried out density functional theory calculations at the B3LYP/6-31+G(*d*) level with Gaussian09 program to examine frontier molecular orbitals (FMOs) of title compounds. FMOs are a key concept in molecular orbital theory, particularly in understanding chemical reactivity and interactions between molecules [36–39]. FMOs denote the highest occupied molecular orbital (HOMO) and the lowest unoccupied molecular orbital (LUMO). These orbitals play a pivotal role in chemical reactivity, as the HOMO contains the most easily donated electrons, while the LUMO represents the most accessible orbital for electron acceptance [40]. Table 2 presents the spatial distribution and energy levels of the HOMO and LUMO orbitals for compounds **AE1**–**AE3**, calculated at the B3LYP/6-31G(*d*) level of theory. According to the theoretical data in Table 2, both HOMO and LUMO are predominantly localized on the aromatic ring in **AE1** and **AE2**, whereas in **AE3**, these orbitals

Table 2. Optimized structures, FMOs, chemical reactivity descriptors (E_g , η , S , χ (in eV)), and dipole moment (μ , in D) of **AE1**, **AE2**, and **AE3** at the B3LYP/6-31+G(*d*) level

Compound	HOMO map and energy values	LUMO map and energy values	E_g , η , S , and μ values
AE1	 -6.9226 eV	 -2.1062 eV	$I = 6.9226$ $A = 2.1062$ $E_g = 4.8164$ $\eta = 2.4082$ $S = 0.4153$ $\chi = 4.5144$ $\mu = 1.8769$
AE2	 -7.2170 eV	 -2.6499 eV	$I = 7.2170$ $A = 2.6499$ $E_g = 4.5671$ $\eta = 2.2836$ $S = 0.4379$ $\chi = 4.9335$ $\mu = 3.3386$
AE3	 -6.9702 eV	 -1.0384 eV	$I = 6.9702$ $A = 1.0384$ $E_g = 5.9318$ $\eta = 2.9659$ $S = 0.3372$ $\chi = 4.0043$ $\mu = 2.0756$

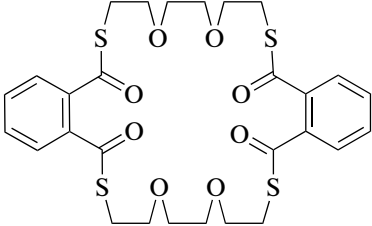
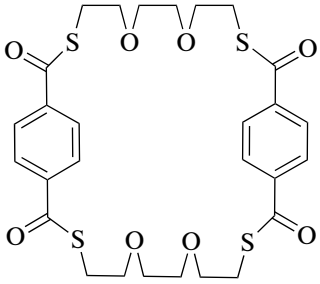
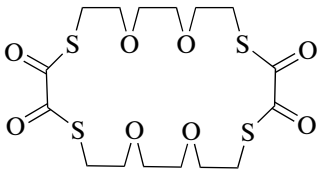
are mainly concentrated around the carbonyl functional group, which can describe most active sides of molecule. Furthermore, electron density within the FMOs exhibits a degree of delocalization across the molecular framework.

To further elucidate the structure–activity relationships, DFT calculations were performed at the B3LYP/6-31+G(*d*) level. Optimized geometries confirmed the expected macrocyclic frameworks, and HOMO–LUMO energy gaps (E_g) were calculated to estimate ligand reactivity. **AE3** exhibited the largest energy gap (5.93 eV), indicating lower chemical reactivity and greater stability. The calculated chemical hardness (η), softness (S), and electronegativity (χ) supported the observed trends in metal ion binding: **AE1** and **AE2**, being softer ($\eta = 2.41$ and 2.28 eV,

respectively), preferentially coordinated softer ions like Ag^+ , while **AE3** favored harder metal ions.

This investigation focused on determining the complexation constants and selectivity factors of previously synthesized mixed-donor thia-crown ethers, which incorporate both hard and soft donor atoms, toward metal ions characterized as hard or soft acids. These parameters were evaluated using the liquid-liquid ion-pair extraction technique, employing chloroform and dichloromethane as organic solvents (Table 3). The observed extraction efficiencies and metal ion selectivities were subsequently analyzed in relation to the ionic radii of the metal cations, the intramolecular sulfur/oxygen heteroatom ratio of the macrocyclic ligands, and the hardness parameters of both the ligands and the metal ions, as conceptualized within

Table 3. Extraction efficiencies of **AE1**, **AE2**, and **AE3** toward selected metal ions in chloroform and dichloromethane, and their relationship to metal–ligand hardness parameters

Thia-crown ether	η_{Metal} , eV ^a	η_{Ligand} , eV ^b	$\Delta\eta$, eV ^c	Ext% (CHCl ₃)	Ext% (CH ₂ Cl ₂)
 AE1: C ₂₈ H ₃₂ O ₈ S ₄	Mg ²⁺ : 32.55 Na ⁺ : 21.08 Ca ²⁺ : 19.52 K ⁺ : 13.64 Zn ²⁺ : 10.88 Fe ²⁺ : 7.24 Ag ⁺ : 6.96	2.41	Mg ²⁺ : 30.14 Na ⁺ : 18.67 Ca ²⁺ : 17.11 K ⁺ : 11.23 Zn ²⁺ : 8.41 Fe ²⁺ : 4.83 Ag ⁺ : 4.55	Zn ²⁺ = K ⁺ > Ag ⁺ > Fe ²⁺ > Mg ²⁺ > Ca ²⁺ > Na ⁺	K ⁺ > Zn ²⁺ > Ag ⁺ > Fe ²⁺ > Mg ²⁺ > Na ⁺ > Ca ²⁺
 AE2: C ₂₈ H ₃₂ O ₈ S ₄	Mg ²⁺ : 32.55 Na ⁺ : 21.08 Ca ²⁺ : 19.52 K ⁺ : 13.64 Zn ²⁺ : 10.88 Fe ²⁺ : 7.24 Ag ⁺ : 6.96	2.28	Mg ²⁺ : 0.27 Na ⁺ : 18.80 Ca ²⁺ : 17.24 K ⁺ : 11.36 Zn ²⁺ : 8.60 Fe ²⁺ : 4.96 Ag ⁺ : 4.68	Zn ²⁺ = K ⁺ > Ag ⁺ > Fe ²⁺ > Ca ²⁺ > Mg ²⁺ > Na ⁺	K ⁺ > Zn ²⁺ > Mg ²⁺ > Ag ⁺ > Fe ²⁺ > Ca ²⁺ > Na ⁺
 AE3: C ₁₆ H ₂₄ O ₈ S ₄	Mg ²⁺ : 32.55 Na ⁺ : 21.08 Ca ²⁺ : 19.52 K ⁺ : 13.64 Zn ²⁺ : 10.88 Fe ²⁺ : 7.24 Ag ⁺ : 6.96	2.97	Mg ²⁺ : 29.58 Na ⁺ : 18.11 Ca ²⁺ : 16.55 K ⁺ : 10.67 Zn ²⁺ : 7.91 Fe ²⁺ : 4.27 Ag ⁺ : 3.99	Zn ²⁺ = K ⁺ > Ag ⁺ > Mg ²⁺ > Ca ²⁺ > Fe ²⁺ > Na ⁺	K ⁺ > Ag ⁺ > Zn ²⁺ > Fe ²⁺ > Mg ²⁺ > Na ⁺ > Ca ²⁺

^a η_{Metal} values (eV) from [5, 6, 19].

^b η_{Ligand} values (eV) calculated at the B3LYP/6-31+G(d) level.

^c $\Delta\eta = \eta_{\text{Metal}} - \eta_{\text{Ligand}}$.

the framework of the Hard-Soft Acid-Base (HSAB) theory, which helps predict the stability of chemical compounds and the direction of chemical reactions, particularly in coordination and inorganic chemistry [5].

According to HSAB theory, sulfur-containing ligands such as thiocrowns exhibit a preference for soft and borderline metal ions, such as Ag⁺ and Zn²⁺ [6]. This was confirmed experimentally, as **AE1** and **AE2** demonstrated high extraction for these cations. On the other hand, **AE3**, with the highest calculated global hardness ($\eta = 2.97$ eV), showed increased extraction of harder ions like Mg²⁺ and Fe²⁺, which is consistent with HSAB predictions and electronic compatibility [5, 19].

The extraction efficiencies were further analyzed in the context of the hardness difference between the metal and ligand ($\Delta\eta = \eta_{\text{metal}} - \eta_{\text{ligand}}$). The results are consistent with the HSAB principle, as a clear trend is observed where metal ions with smaller absolute hardness differences ($|\Delta\eta|$) generally exhibit higher

extraction percentages [19]. This is evident, for example, in the data for **AE2** (Tables 1–3), where the high extraction efficiencies for K⁺ and Zn²⁺ correspond to some of the smallest $|\Delta\eta|$ values. This consistent pattern across the ligand series strongly supports the premise that minimal hardness difference favors stronger binding and more efficient extraction.

The metal complexation behavior of the **AE1**–**AE3** compounds was investigated using liquid–liquid ion pair extraction, considering factors such as the hardness of the ligands, the hardness of the metal ions, and the heteroatom (S/O) ratio. Although **AE1**, **AE2**, and **AE3** share an identical sulfur-to-oxygen ratio (S/O = 0.5), their extraction efficiencies in dichloromethane and chloroform exhibit slight variations, as reflected in their respective extraction percentages (Table 3). These differences can be attributed to the varying polarities of the two solvents. While the sulfur atoms in the thiocrown ring introduce steric hindrance, their uniform positions across all three compounds minimize their impact on metal complexation. Notably,

AE1 and **AE2** are structural isomers, which contribute to their differing polarity-related properties, including hardness. In these isomers, the carbonyl substituents are attached to the benzene ring at the 1,2-position in **AE1** and the 1,4-position in **AE2**. However, the thia-crown ether ring formed via oxalyl chloride cyclization also favors the 1,2-position, thereby influencing the cavity size and internal spatial arrangement of the **AE2** compound.

AE3 has the highest η (2.97 eV), making it a harder base compared to **AE1** and **AE2**. Therefore, **AE3** shows relatively higher extraction for hard metal ions such as Mg^{2+} and Fe^{2+} . In contrast, **AE1** and **AE2**, being softer ($\eta = 2.41$ and 2.28 , respectively), prefer softer or borderline acids like K^+ , Zn^{2+} , and Ag^+ . $\Delta\eta$ values ($\eta_{\text{metal}} - \eta_{\text{ligand}}$) also reflect the expected trend: smaller $\Delta\eta$ implies better electronic matching and thus higher extraction, as seen with Zn^{2+} and K^+ . Additionally, the DFT-calculated HOMO–LUMO energy gaps (E_g) further support this: **AE3**'s higher E_g suggests greater chemical stability and reduced reactivity, aligning with its lower affinity for softer ions.

CONCLUSIONS

In this study, three thia-crown ether derivatives (**AE1**, **AE2**, and **AE3**) were synthesized and characterized for their ability to complex with various biologically and environmentally relevant metal ions. Their extraction efficiencies were systematically examined in chloroform and dichloromethane solvent systems using liquid–liquid ion-pair extraction techniques. All ligands exhibited high affinity for K^+ and Zn^{2+} , consistent with their cavity size compatibility and the electronic matching predicted by the HSAB principle.

Across both solvents, K^+ , Zn^{2+} , and Ag^+ consistently exhibit high extraction efficiencies, particularly by **AE1** and **AE2**. For example, **AE2** extracts Zn^{2+} and K^+ at the rate of 98.2% in chloroform, suggesting strong complexation affinity. Conversely, Na^+ and Ca^{2+} ions generally exhibit lower extraction values, likely due to size mismatch and harder acid character. In both solvent systems, **AE1** and **AE2** consistently exhibit a preference for K^+ and Zn^{2+} over Ag^+ , suggesting that these ligands preferentially bind cations characterized by intermediate hardness and relatively larger ionic radii.

Dichloromethane, being slightly more polar than chloroform, enhances the extraction efficiency of K^+ ions—reaching up to 99.5%—while reducing the extraction of certain other ions such as Ca^{2+} and Na^+ , depending on the specific ligand involved. These findings underscore the significant role of solvent polarity in governing metal–ligand interactions and the distribution of metal ions between phases.

Notably, Na^+ displays the weakest interaction with all ligands, despite belonging to the same group as K^+ .

This behavior is likely attributed to its smaller ionic radius (102 pm compared to 138 pm for K^+), resulting in a less favorable fit within the macrocyclic cavity. Likewise, the moderate extraction efficiencies observed for Fe^{2+} and Mg^{2+} align with their classification as harder Lewis acids. The lack of pronounced selectivity in chloroform, contrasted with the enhanced selectivity—particularly for K^+ —observed in dichloromethane, indicates that solvent selection plays a pivotal role in modulating both binding affinity and ion-size compatibility within the ligand cavity.

Theoretical calculations, including DFT-based evaluations of HOMO–LUMO gaps and hardness parameters, reinforced the experimental findings. Ligand hardness and metal–ligand hardness compatibility ($\Delta\eta$) strongly influenced extraction performance and selectivity. Among the title compounds, **AE2** demonstrated the most balanced selectivity and efficiency profile.

In light of the obtained results, it has been observed that thia-crown ether derivatives with biological significance can successfully extract and remove K^+ , Ca^{2+} , Na^+ , Ag^+ , Fe^{2+} , Zn^{2+} , and Mg^{2+} ions from biological and environmental aqueous solutions. The combined experimental and theoretical data on the synthesized compounds validate the fundamental utility of thia-crown ethers as versatile ligands for selective metal ion recognition. The insights gained into the roles of cavity size, hardness, and solvent effects provide a strong foundation for future work, which could explore re-extraction processes and lead to potential applications in sensing and environmental remediation.

SUPPLEMENTARY INFORMATION

The online version contains supplementary material available at <https://doi.org/10.1134/S1990793125701763>.

FUNDING

BÇ appreciate that this work was supported by Balikesir University Research Grant no. 2025/211. AA gratefully acknowledges that this work was supported by Balikesir University Research Grant no. 2020/037.

CONFLICT OF INTEREST

The authors of this work declare that they have no conflicts of interest.

REFERENCES

1. C. J. Pedersen, *J. Am. Chem. Soc.* **89**, 7017 (1967). <https://doi.org/10.1021/ja01002a035>
2. J. S. Bradshaw, K. E. Krakowiak, and R. M. Izatt, *Aza-Crown Macrocycles: An Overview* (John Wiley and Sons, New York, 1993). <https://doi.org/10.1002/9780470187388.ch1>

3. S. N. Dmitrieva, M. V. Churakova, N. A. Kurchavov, A. I. Vedernikov, A. Y. Freidzon, S. S. Basok, A. A. Bagatur'yants, and S. P. Gromov, *Russ. J. Org. Chem.* **47**, 1101 (2011).
<https://doi.org/10.1134/S1070428011070220>
4. V. F. Gromov, G. N. Gerasimov, M. I. Ikim, E. Y. Spiridonova, and L. I. Trakhtenberg, *Russ. J. Phys. Chem. B* **14**, 492 (2020).
<https://doi.org/10.1134/S1990793120030045>
5. R. G. Parr and R. G. Pearson, *J. Am. Chem. Soc.* **105**, 7512 (1983).
<https://doi.org/10.1021/ja00364a005>
6. R. G. Pearson, *Inorg. Chem.* **27**, 734 (1988).
<https://doi.org/10.1021/ic00277a030>
7. H. T. Fissaha, G. M. Nisola, F. K. Burnea, J. Y. Lee, S. Koo, S. P. Lee, K. Hern, and W. J. Chung, *J. Ind. Eng. Chem.* **81**, 415 (2020).
<https://doi.org/10.1016/j.jiec.2019.09.032>
8. L. F. Lindoy, *The Chemistry of Macrocyclic Ligand Complexes* (Cambridge Univ. Press, Cambridge, 1975).
9. S. R. Cooper, W. B. Jones, and S. C. Rawle, *Compr. Heterocycl. Chemistry II* **1**, 843 (1996).
<https://doi.org/10.1016/B978-008096518-5.00238-0>
10. B. Çiçek and Ü. Çalıřır, *Lett. Org. Chem.* **13**, 572 (2016).
<https://doi.org/10.2174/15701786136661609061053>
11. T. Schneider, N. Brüssow, A. Yuvanc, and N. Budisa, *ChemistrySelect* **5**, 2854–2857 (2020).
<https://doi.org/10.1002/slct.202000122>
12. B. Çiçek, A. Ergun, and N. Gençer, *Asian J. Chem.* **24**, 3729 (2012).
13. A. Yordanov and D. M. Roundhill, *Coord. Chem. Rev.* **170**, 93 (1998).
[https://doi.org/10.1016/S0010-8545\(97\)00074-X](https://doi.org/10.1016/S0010-8545(97)00074-X)
14. B. Çiçek and Z. Onbařıođlu, *Heterocycl. Commun.* **22**, 329 (2016).
<https://doi.org/10.1515/hc-2016-0097>
15. L. A. Litvinova and A. V. Anisimov, *Russ. Chem. Bull.* **48**, 473 (1999).
<https://doi.org/10.1007/BF02251813>
16. Ü. Çakir and B. Çiçek, *Transit. Metal Chem.* **29**, 263 (2004).
<https://doi.org/10.1023/B:TMCH.0000020358.69194.82>
17. M. H. Mashhadizadeh, A. Mostafavi, N. Razavi, and M. Shamsipur, *Talanta* **58**, 1009 (2002).
[https://doi.org/10.1016/S0039-9140\(02\)00398-4](https://doi.org/10.1016/S0039-9140(02)00398-4)
18. H. Alp, Z. Bıyıklıođlu, M. Ocak, Ü. Ocak, H. Kantekin, and G. Dilber, *Sep. Sci. Technol.* **42**, 835 (2007).
<https://doi.org/10.1080/01496390601174000>
19. B. Srivastava, M. K. Barman, and B. Mandal, *Desalination Water Treat.* **53**, 398 (2015).
<https://doi.org/10.1080/19443994.2013.841101>
20. L. M. Abbass, S. A. Sadeek, W. A. Zordok, M. Abdelaziz, and M. S. El-Attar, *J. Mol. Struct.* **1308**, 138115 (2024).
<https://doi.org/10.1016/j.molstruc.2024.138115>
21. M. Gvozdev, I. Turomsha, N. Osipovich, and N. Loginova, *J. Biol. Inorg. Chem.* **30**, 257 (2025).
<https://doi.org/10.1007/s00775-025-02107-y>
22. A. A. Alezzy, S. A. Al-horaibi, H. A. Alnahari, A. B. Al-Odayni, M. ALSaeedy, A. AL-Adhrai, W. Saeed, G. Alshawesh, and P. M. Arif, *J. Mol. Struct.* **1299**, 137069 (2024).
<https://doi.org/10.1016/j.molstruc.2023.137069>
23. I. M. Smallwood, *Handbook of Organic Solvent Properties* (Butterworth-Heinemann, Oxford, 2012).
<https://doi.org/10.1016/C2009-0-23646-4>
24. Ü. Çakir, Y. K. Yildiz, and M. Alkan, *J. Incl. Phenom. Macrocycl. Chem.* **34**, 155 (1999).
<https://doi.org/10.1023/A:1017114408086>
25. M. J. Frisch, G. W. Trucks, H. B. Schlegel, G. E. Scuseria, M. A. Robb, J. R. Cheeseman, G. Scalmani, V. Barone, G. A. Petersson, H. Nakatsuji, X. Li, M. Caricato, A. V. Marenich, J. Bloino, B. G. Janesko, R. Gomperts, B. Mennucci, H. P. Hratchian, J. V. Ortiz, A. F. Izmaylov, J. L. Sonnenberg, D. Williams-Young, F. Ding, F. Lipparini, F. Egidi, J. Goings, B. Peng, A. Petrone, T. Henderson, D. Ranasinghe, V. G. Zakrzewski, J. Gao, N. Rega, G. Zheng, W. Liang, M. Hada, M. Ehara, K. Toyota, R. Fukuda, J. Hasegawa, M. Ishida, T. Nakajima, Y. Honda, O. Kitao, H. Nakai, T. Vreven, K. Throssell, J. A. Montgomery, J. E. Peralta, F. Ogliaro, M. J. Bearpark, J. J. Heyd, E. N. Brothers, K. N. Kudin, V. N. Staroverov, T. A. Keith, R. Kobayashi, J. Normand, K. Raghavachari, A. P. Rendell, J. C. Burant, S. S. Iyengar, J. Tomasi, M. Cossi, J. M. Millam, M. Klene, C. Adamo, R. Cammi, J. W. Ochterski, R. L. Martin, K. Morokuma, O. Farkas, J. B. Foresman, and D. J. Fox, *Gaussian 09, Revision A.02* (Gaussian, Inc., Wallingford CT, 2009).
26. A. D. Becke, *J. Chem. Phys.* **98**, 5648 (1993).
<https://doi.org/10.1063/1.464913>
27. C. Lee, W. Yang, and R. G. Parr, *Phys. Rev. B* **37**, 785 (1988).
<https://doi.org/10.1103/PhysRevB.37.785>
28. R. Kurtaran, S. Odabařıođlu, A. Azizoglu, H. Kara, and O. Atakol, *Polyhedron* **26**, 5069 (2007).
<https://doi.org/10.1016/j.poly.2007.07.021>
29. S. M. Mohammed, W. Shehta, A. H. Moustafa, A. M. Salem, A. A. Masry, and H. A. El-Sayed, *Russ. J. Gen. Chem.* **94**, 3003 (2024).
<https://doi.org/10.1134/S1070363224110239>
30. F. Mollaamin and M. Monajjemi, *Russ. J. Phys. Chem. B* **19**, 1 (2025).
<https://doi.org/10.1134/S1990793124701501>
31. D. Badrzadeh, R. Ahmadi, S. Sheshmani, S. K. Moghadamb and A. S. Shahvelayati, *Russ. J. Phys. Chem. B* **19**, 193 (2025).
<https://doi.org/10.1134/S1990793124701653>
32. A. Franklin Ebenazer, M. Saravanabhavan, K. S. Ramesh, S. Muhammad, A. G. Al-Sehemi, and N. Sampathkumar, *J. Phys. Chem. Solids* **170**, 110886 (2022).
<https://doi.org/10.1016/j.jpcs.2022.110886>
33. F. Jensen, *Introduction to Computational Chemistry* (John Wiley and Sons, West Sussex, 1999).
34. R. D. Shannon, *Acta Crystallogr. A* **32**, 751 (1976).
<https://doi.org/10.1107/S0567739476001551>
35. L. G. A. V. Water, W. L. Driessen, M. W. Glenny, J. Reedijk, and M. Schröder, *React. Funct. Polym.* **51**,

- 33 (2002).
[https://doi.org/10.1016/S1381-5148\(02\)00031-7](https://doi.org/10.1016/S1381-5148(02)00031-7)
36. Z. Özer, T. Kılıç, S. Çarıkçı, and A. Azizoglu, *Russ. J. Phys. Chem.* **93**, 2703 (2019).
<https://doi.org/10.1134/S0036024419130235>
37. A. V. P. D. Aroquiaraj, K. S. Satheeshkumar, G. Bouzid, P. Francisxavier, and A. Sahbi, *Vietnam J. Chem.* (2025) (in press).
<https://doi.org/10.1002/vjch.70025>
38. H. Chekroud, A. Bouhadiba, N. Naili, A. Benaïssa, N. F. Djazi, and S. Heddami, *Russ. J. Org. Chem.* **61**, 162 (2025).
<https://doi.org/10.1134/S1070428024603297>
39. Y. Tian, W. Chen, Z. Zhao, L. Xu, and B. Tong, *J. Mol. Model.* **26**, 67 (2020).
<https://doi.org/10.1007/s00894-020-4325-8>
40. I. Fleming, *Frontier Orbitals and Organic Chemical Reactions* (Oxford Univ. Press, Oxford, 2010).
<https://doi.org/10.1002/9780470689493>

Publisher's Note. Pleiades Publishing remains neutral with regard to jurisdictional claims in published maps and institutional affiliations. AI tools may have been used in the translation or editing of this article.